Molecular Biology of the Cell
Vol. 20, 4140–4152, October 1, 2009

Caveolae Mediate Growth Factor-induced Disassembly of Adherens Junctions to Support Tumor Cell Dissociation

Lidiya Orlichenko,*† Shaun G. Weller,*† Hong Cao,* Eugene W. Krueger,* Muyiwa Awoniyi,* Galina Beznoussenko,‡ Roberto Buccione,‡ and Mark A. McNiven*

*Mayo Clinic, Department of Biochemistry and Molecular Biology and the Miles and Shirley Fiterman Center for Digestive Diseases, Rochester, MN 55905; and ‡Consorzio Mario Negri Sud, Santa Maria Imbaro (Chieti) 66030, Italy

Submitted October 17, 2008; Revised July 6, 2009; Accepted July 22, 2009
Monitoring Editor: Keith E. Mostov

Remodeling of cell–cell contacts through the internalization of adherens junction proteins is an important event during both normal development and the process of tumor cell metastasis. Here we show that the integrity of tumor cell–cell contacts is disrupted after epidermal growth factor (EGF) stimulation through caveolae-mediated endocytosis of the adherens junction protein E-cadherin. Caveolin-1 and E-cadherin closely associated at cell borders and in internalized structures upon stimulation with EGF. Furthermore, preventing caveolae assembly through reduction of caveolin-1 protein or expression of a caveolin-1 tyrosine phospho-mutant resulted in the accumulation of E-cadherin at cell borders and the formation of tightly adherent cells. Most striking was the fact that exogenous expression of caveolin-1 in tumor cells that contain tight, well-defined, borders resulted in a dramatic dispersal of these cells. Together, these findings provide new insights into how cells might disassemble cell–cell contacts to help mediate the remodeling of adherens junctions, and tumor cell metastasis and invasion.

INTRODUCTION

Polarized epithelial cells such as those in ductular organs, including the pancreas, form and maintain their tubular tissue architecture through regulated associations with adjacent cells (Hogan and Kolodziej, 2002; Lubarsky and Krasnow, 2003; Zegers *et al.*, 2003). The integrity of these lateral interactions is mediated, in part, by adherens junctions (AJs), of which the transmembrane protein E-cadherin (E-cad) is a major component. On the extracellular side, homophilic antiparallel interactions between E-cad molecules present on adjacent cells mediate the assembly and maintenance of AJs, whereas on the intracellular side the cytoplasmic tail of E-cad is associated with an array of actin cytoskeletal proteins as well as signaling molecules such as catenins, small GTPases, and nonreceptor tyrosine kinases (Perez-Moreno *et al.*, 2003; Gumbiner, 2005). Although maintenance of stable junctions is important for tissue integrity and the functional properties of polarized epithelia, AJs are also dynamic structures undergoing cycles of assembly and disassembly. Indeed, reorganization of AJs is a key aspect of tissue morphogenesis both during normal development as well as tumor cell metastasis, when the structural integrity of AJs is compromised as tumor cells lose polarity and subsequently dissociate before migration (Thiery, 2002; Cavallaro and Christofori, 2004).

Pancreatic cancer is a particularly deadly disease and is listed as one of the top five most lethal cancers in the United States (Jemal *et al.*, 2006). Although less prevalent than other cancers, its mortality rate is well over 90% within 6 mo of diagnosis. This exceptionally high lethality is due to a lack of early diagnostic tools, the dispersed organization of the pancreas within the abdomen, and a significant propensity of neoplastic cells to disseminate and migrate from the pancreas to nearby organs (Shi *et al.*, 2001; Freelove and Walling, 2006).

A reduction in E-cad protein has been implicated as a prerequisite for migratory activity and the development of an invasive metastatic phenotype in pancreatic cancers (Imamichi *et al.*, 2007). It has also been described as an independent prognostic factor for patient survival (Karayiannakis *et al.*, 2001; Garcea *et al.*, 2005). Indeed, the loss of E-cad expression has been shown to facilitate peritoneal dissemination of pancreatic cancer cells (Furuyama *et al.*, 2000) and has been found to be associated with high-grade and advanced-stage pancreatic tumors (Pignatelli *et al.*, 1994). In contrast, several recent studies have demonstrated that pancreatic carcinomas maintain normal levels of E-cad (Menke *et al.*, 2001; Alldinger *et al.*, 2005; Toyoda *et al.*, 2005), suggesting that additional mechanisms of tumor cell dissemination also exist (see Cavallaro and Christofori, 2004).

It is known that stimulation of cells with growth factors can affect the stability of AJs by altering the internalization and vesicle trafficking dynamics of E-cad. However, the precise endocytic mechanisms used remain unclear, as both clathrin- and caveolae-mediated endocytosis have been implicated in growth factor–stimulated internalization of AJ components (Bryant and Stow, 2004; D'Souza-Schorey, 2005; Ivanov *et al.*, 2005). As examples, in hepatocyte growth

This article was published online ahead of print in *MBC in Press* (http://www.molbiolcell.org/cgi/doi/10.1091/mbc.E08–10–1043) on July 29, 2009.

† These authors contributed equally to this work.

Address correspondence to: Mark A. McNiven (mcniven.mark@mayo.edu).

Abbreviations used: AJ, adherens junction; Cav1, caveolin-1; E-cad, E-cadherin; PM, plasma membrane; siRNA, small interfering RNA; TER, transepithelial electrical resistance.

factor–treated Madin-Darby canine kidney (MDCK) cells, a clathrin-dependent pathway was suggested to mediate E-cad internalization from the basolateral domain (Palacios *et al.*, 2002) before degradation in a lysosomal compartment (Palacios *et al.*, 2005). Similarly, clathrin-mediated endocytosis and subsequent lysosomal degradation of E-cad has also been implicated in mouse mammary epithelial cells treated with TGFβ in combination with sustained activation of Raf; however, a caveolin-mediated pathway was not ruled out (Janda *et al.*, 2006). Finally, epidermal growth factor (EGF) signaling in A431 epidermoid carcinoma cells was shown to trigger E-cad endocytosis by a clathrin-independent pathway that was sensitive to cholesterol depletion, possibly via caveolae (Lu *et al.*, 2003). Thus, the endocytic mechanism used to internalize E-cad might vary depending on cell type as well as specific types of growth factor stimulation.

We have recently reported that normal epithelial cells as well as pancreatic tumor cells form exceptionally large numbers of caveolae at cell borders in response to EGF treatment (Orlichenko *et al.*, 2006). Caveolae are small flask-shaped endocytic structures of 50–90 nm in diameter rich in cholesterol and sphingolipids while also containing a protein coat of caveolin oligomers. Caveolae not only mediate the internalization of a variety of cargo molecules, rather caveolae and caveolin membrane domains may also represent compartmentalized signaling platforms (Liu *et al.*, 2002; Pelkmans and Helenius, 2002; Parton *et al.*, 2006; Parton and Simons, 2007). Indeed, the dramatic assembly of caveolae structures we observed in EGF-stimulated cells appears to be dependent upon Src-mediated phosphorylation of a specific tyrosine residue (Y14) at the N-terminus of caveolin-1 (Cav1; Li *et al.*, 1996; Lee *et al.*, 2000; Orlichenko *et al.*, 2006). Caveolae formation occurs rapidly in stimulated cells at the onset of AJ disassembly; thus, we hypothesized that caveolae could represent the endocytic pathway used by activated cells to internalize E-cad and other AJ components.

In this present study we provide direct evidence suggesting an active role for caveolae formation in the internalization of E-cad from the borders of EGF-stimulated MDCK cells and pancreatic tumor cells (BxPC-3, PANC-1, and HPAF-II). Cav1 and E-cad colocalized at cell borders under resting conditions, but were internalized and transported together after EGF treatment, accumulating at large cytoplasmic vesicles coated with Cav1. Concomitant with this morphological cointernalization was an enhanced physical interaction between Cav1 and E-cad, as indicated by coimmunoprecipitation of these proteins. When testing for a direct role of caveolae formation in AJ internalization, we found that expression of a RFP red fluorescent protein (RFP)-tagged Cav1 tyrosine phospho-mutant (Cav1Y14F-mRFP) or reduction of Cav1 protein levels by small interfering RNA (siRNA) treatment significantly increased the levels of E-cad at AJs. Consistent with this retention of E-cad at cell borders, MDCK cells stably expressing Cav1Y14F-mRFP formed tightly packed cell colonies with extended cell–cell contacts and exhibited an increase in transepithelial electrical resistance (TER). Finally, we observed that different pancreatic tumor cell types exhibit an intrinsic inverse correlation in Cav1 and E-cad protein levels. Moreover, when Cav1 levels are increased by exogenous expression of Cav1 in cells that normally express low levels of Cav1, the ability of these cells to disseminate is dramatically altered. Together, these findings provide strong support for the concept that caveolae play a role in the internalization of AJ proteins such as E-cad and subsequent disassembly of cell–cell contacts. The implications of Cav1 expression and caveolae formation in the metastasis of pancreatic tumor cells are discussed.

MATERIALS AND METHODS

Cells

Human neoplastic pancreatic ductular epithelial cells (PANC-1, BxPC-3, and HPAF-II) and normal MDCK epithelial cells were from American Type Culture Collection (Rockville, MD). PANC-1 cells were maintained in DMEM (Mediatech, Herndon, VA) supplemented with 10% FBS (Invitrogen, Carlsbad, CA) and 5% FCS, respectively. MDCK cells were maintained in EMEM (Mediatech) containing 10% FBS. BxPC-3 cells were grown in RPMI 1640 (Mediatech) containing 10% FBS and supplemented with glutamine, 10 mM HEPES, 4.5 mM glucose, and 1.5 mM sodium bicarbonate. HPAF-II cells were maintained in EMEM containing 10% FBS and supplemented with 0.1 mM nonessential amino acids and 1 mM sodium pyruvate. Media for all cell lines contained 50 μg/ml penicillin and 50 μg/ml streptomycin (Invitrogen, Carlsbad, CA). All cells were grown at 37°C in 5% CO_2. Cells were grown in plastic tissue culture dishes for biochemical analyses, on acid-washed coverslips for fluorescence microscopy, and on carbon-coated and glow-discharged gridded coverslips (Bellco Glass, Vineland, NJ) for electron microscopy (EM).

Antibodies and Constructs

The anti-caveolin-1 (Cav1) polyclonal antibodies were generated in rabbits injected with a peptide comprising a sequence present in the N-terminus of rat α-Cav1 (amino acids 5–33: KYVDSEGHLYTVPIREQGNIYKPNNKAMA) and affinity-purified as previously described (Henley and McNiven, 1996). Monoclonal anti-Cav1 and anti-Cav1 PY14 antibodies were purchased from Transduction Laboratories (Lexington, KY); the monoclonal anti-E-cadherin antibody was from BD Biosciences (San Jose, CA); the anti-ZO-1 antibody was from Santa Cruz Biotechnology, (Santa Cruz, CA); the Src, Erk1/2, active-Src and Erk antibodies were from Cell Signaling Technology (Danvers, MA). Secondary goat anti-rabbit and goat anti-mouse IgG antibodies linked to horseradish peroxidase were from Invitrogen. Fluorescently-conjugated secondary goat anti-rabbit and goat anti-mouse antibodies were from Invitrogen. Cav1 was PCR-amplified from rat liver cDNA using the following primers containing HindIII (forward) and EcoRI (reverse) restriction enzyme sites: forward: 5′-AAGCTTAG-CATGTCTGGGGGTAAATACGTAGAC-3′; and reverse 5′-GAATTCCCT-GAAATGTCAC-3′.

The PCR product was digested with the appropriate restriction enzymes and cloned into the pEGFP-N_1 vector (Clontech, Palo Alto, CA) to generate the Cav1-GFP construct. This construct was then used as template along with the Stratagene QuickChange Site-Directed Mutagenesis kit (Stratagene, La Jolla, CA) to generate the Cav1Y14F-GFP construct. The Cav1Y14F insert was subsequently subcloned into the pDsRed-N_1 vector (mRFP, Clontech) to generate the Cav1Y14F-mRFP construct. The green fluorescent protein (GFP)-tagged version of E-cadherin was a kind gift of W. James Nelson. Constructs were purified using the Qiagen Plasmid Purification kit (Qiagen, Valencia, CA) and sequenced by the Mayo Molecular Biology Core Facility (Mayo Clinic, Rochester, MN). Constructs were verified using the DNASTAR SeqMan program (DNASTAR, Madison, WI).

Generation of Stable Cell Lines

MDCK, BxPC-3, and HPAF-II cells stably expressing fluorescently tagged (mRFP or GFP) wild-type (wt) Cav1 or Cav1Y14F were generated according to a protocol from Bio-Rad (Hercules, CA). Briefly, MDCK, BxPC-3, and HPAF-II cells plated in two 75-ml flasks were allowed to grow until they reached 70% confluency. Cells were then collected into 15-ml tubes and washed three times with ice-cold PBS without disturbing the pellet by spinning cells down in a low-speed centrifuge for 5 min. After that, cells were preincubated with DNA (20 μg/μl) on ice for 10 min, followed by electroporation using the Bio-Rad Gene Pulser II system (Bio-Rad). The transfected cells were then incubated on ice for 10 min, transferred to complete media, and incubated overnight to allow for expression of Cav1. MDCK, BxPC-3, and HPAF-II cells stably expressing wt Cav1-GFP, Cav1Y14F-GFP, or Cav1Y14F-mRFP and resistant to 0.1, 0.15, and 0.4 mg/ml G-418 (Invitrogen), respectively, were selected and used for the described experiments.

Transfection, Fluorescence Microscopy, and EM

The GeneJammer transfection reagent (Stratagene) was used for transfection of pancreatic tumor and normal cells according to the manufacturer's protocol. EGF was from Invitrogen, and EGF treatment of serum-starved cells before processing for fluorescence microscopy was performed as previously described (Orlichenko *et al.*, 2006). Cells were fixed with 3% formaldehyde, washed three times in Dulbecco's PBS (D-PBS), permeabilized in 0.1% Triton for 2 min, blocked for 1 h in blocking buffer (5% goat serum, 5% glycerol, and 0.04% sodium azide in D-PBS), and incubated with primary antibodies, when indicated, for 1 h. Cells were then washed three times in D-PBS for 10 min each followed by a 1-h incubation with secondary antibodies. After that, cells were washed three times in D-PBS for 10 min and mounted in ProLong antifade reagent (Invitrogen). Fluorescence micrographs were acquired using either a Zeiss Axiovert 35 epifluorescence microscope (Carl Zeiss, Thornwood, NJ) equipped with a Hamamatsu Orca II camera (Hamamatsu Pho-

tonics, Hamamatsu City, Japan) or Zeiss LSM510 confocal microscope (Carl Zeiss, Jena, Germany).

Control untransfected MDCK cells or MDCK cells stably expressing Cav1Y14F-mRFP were processed for EM as previously described (Henley *et al.*, 1998) and imaged using a JEOL 1200 electron microscope (JEOL Ltd., Tokyo, Japan) to analyze cell junctions.

Live time-lapse imaging of HPAF-II cells stably expressing wt Cav1-GFP or Cav1Y14F-GFP was performed on a Zeiss Axiovert 35 epifluorescence microscope equipped with a heated stage using a Hamamatsu Orca II camera and IPLab imaging software (Scanalytics, Fairfax, VA). Cells were plated in 35-mm culture dishes containing a glass bottom and viewed with a 63 × 1.4 NA lens. MEM medium (Mediatech) containing 10% FBS and buffered with 15 mM HEPES (pH 7.2) was used for imaging. Five minutes before imaging, cells were stimulated with 30 ng/ml EGF. Images were acquired every 15 s using a 500-ms exposure time over a 25-min time period. Alternatively, time-lapse studies were performed on PANC1 cells using a Zeiss LSM 510 confocal microscope.

3D Reconstruction of Images

For images rendered in 3D, EGF-stimulated HPAF-II cells grown on glass coverslips were fixed, permeabilized in 0.2% Triton, costained with antibodies against Cav1 and E-cadherin (E-cad), and imaged using a Zeiss LSM510 confocal microscope. At least 23 slices were acquired per image at 3-μm intervals, and 3D reconstruction was performed using LSM510 software.

Measurement of TER

To determine TER, untransfected MDCK cells or MDCK cells stably expressing GFP, wt Cav1-GFP, or Cav1Y14F-mRFP were seeded on BD Falcon cell culture inserts with an 8-μm pore size (Franklin Lakes, NJ) and allowed to reach confluency. Measurements were subsequently taken 24 and 48 h after confluency using a Millipore Millicell-ERS resistance system (Billerica, MA). After subtracting the background resistance value of a blank filter in medium, all values were normalized to filter size.

Caveolin-1 Knockdown via siRNA

SiRNA duplexes targeting human Cav1 mRNA as well as a control scrambled siRNA were purchased from Dharmacon (Lafayette, CO), and cells were transfected according to the manufacturer's instructions. Briefly, cells seeded on coverslips (for fluorescence microscopy) or on 10-cm tissue culture dishes (for biochemical assays) were grown under normal conditions until they reached 30–50% confluency. Cells were then washed in low serum OPTI-MEM medium (Invitrogen) and transfected with 75 μM Cav1 siRNA using Oligofectamine reagent (Invitrogen). Five hours after transfection, an equal volume of medium containing 30% FBS was added to the OPTI-MEM, and cells were allowed to recover for the time specified in the corresponding figure legends (from 24 to 72 h). The siRNA sequence targeting human Cav1 was AACCAGAAGGGACACACAGUU, a sequence previously shown to effectively knockdown Cav1 expression (Cho *et al.*, 2003; Orth *et al.*, 2006).

Immunoprecipitation, Biotinylation Studies, SDS-PAGE, and Western Blotting

Immunoprecipitation of Cav1, SDS-PAGE, and Western blotting were performed as previously described (Orlichenko *et al.*, 2006). A stripping protocol was used for assessment of protein expression levels of E-cad, Cav1, and PY14 Cav1 on the same membrane. For stripping, 20 ml of stripping buffer (14.6 ml H_2O, 4 ml 10% SDS, 139 μl MeOH, and 1.125 ml 1 M Tris-HCl, pH 7.0) was applied to the membrane and incubated at 50°C for 30 min. The membrane was then washed two times for 10 min each with D-PBS containing 0.05% Tween 20 (D-PBST) and reblocked with 5% fat free milk in D-PBST. Horseradish peroxidase (HRP)-conjugated secondary antibodies were detected using ECL reagents (Amersham, Arlington Heights, IL) according to the manufacturer's instructions.

To determine the level of internalized E-cad protein in the MDCKts-VSrc cell line after v-Src activation, a cell surface biotinylation assay was performed essentially as described previously (Cao *et al.*, 2005). After the biotin labeling of surface protein, cells were lysed and E-cad protein was immunoprecipitated using a commercially available mAb (BD Biosciences). The ratio of biotinylated surface Ecadherin levels to that of total immunoprecipitated protein was compared with or without a 7-h shift to the permissive temperature to activate v-Src. Sulfo-NHS-LC-biotin and HRP-conjugated streptavidin were from Pierce (Rockford, IL).

Quantitative Analysis

Quantitative analysis of randomly selected fields of cells was performed using IPLab imaging software on images acquired using a Zeiss Axiovert 35 epifluorescence microscope. The level of E-cad staining at individual cell junctions was measured by plotting the signal intensity along a linear cross-sectional image trace that incorporated multiple cell junctions. The average intensity of E-cad signal for individual cell borders was calculated by averaging the intensity for registered pixels within regions of cell junctions. Analysis of E-cad localized at cell junctions was performed on at least 15 cell borders for each experimental condition.

Quantitative analysis of Western blots was performed based on the densitometry of scanned bands using the Bio-Rad Image Analysis System with Molecular Analyst Software and a Bio-Rad Model GS-700 Imaging Densitometer (Bio-Rad). Bands were normalized to a background of the film of equal area and to a loading control.

RESULTS

EGF-induced Caveolae Formation Leads to an Increased Association of Cav1 and E-cad during the Disassembly of Cell Junctions

We and others have observed that Cav1 is highly enriched along the borders of a variety of normal and neoplastic cultured epithelial cells (Palacios *et al.*, 2002; Lu *et al.*, 2003; Janda *et al.*, 2006; Orlichenko *et al.*, 2006; Figure 1, a–c). Interestingly, when resting cells were examined by EM, very few caveolae structures were observed at the peripheral sites where Cav1 protein is concentrated. As shown in the electron micrographs of cultured human pancreatic tumor cells (PANC-1), the borders between adjacent cells are generally intact and display few invaginations (Figure 1d). In dramatic contrast to resting cells, stimulation of cells with EGF (30 ng/ml) for 10–30 min induced a marked assembly of caveolar structures at the plasma membrane (PM), resulting in a loss of cell–cell contacts and separation of adjacent cells (Figure 1e). Assembly of caveolae under these conditions was rapid and extensive, as indicated by the long "caveolar towers" seen extending off the cell borders into the cytoplasm (Figure 1e). In addition, this dramatic assembly of caveolae was observed in polarized epithelial cells (MDCK and normal rat kidney [NRK]) as well as human pancreatic ductular tumor cells (PANC-1 and BxPC-3); therefore, we assume that this phenomenon is exhibited by many epithelial cell types.

Although Cav1 and E-cad showed a marked colocalization at cell borders in resting cells (Figure 1, a–c and a′–c′), whether this localization represented a participation of Cav1 in growth factor-stimulated internalization of AJ proteins or rather was simply coincidental remained to be determined. Therefore, we stimulated MDCK cells, as a control epithelial cell type, and human pancreatic tumor cells (BxPC-3) with EGF for 5–30 min before fixation and immunostaining for Cav1 and E-cad (Figure 2, a–b‴). By 20 min after EGF treatment, a punctate distribution of Cav1 could be noted along the borders between adjacent cells, consistent with the formation of caveolar structures. However, most striking was the formation of large (0.5–2 μm), spherical, intracellular compartments that were coated along the periphery with Cav1 and filled with E-cad (Figure 2, a–b‴). Furthermore, although EGF treatment induced the formation of these structures in MDCK cells and increased their number in BxPC-3 cells, caveolar clusters also formed spontaneously without EGF exposure in the various pancreatic tumor cell types tested (BxPC-3, PANC-1, and HPAF-II; Supplemental Figure S1), consistent with observations by others that pancreatic tumor cells possess amplified signaling pathways (Korc *et al.*, 1992; Yamanaka *et al.*, 1993; Oikawa *et al.*, 1995; Liu *et al.*, 1998; Alldinger *et al.*, 2005).

In support of the observations described above gathered from static images, dual-color time-lapse confocal microscopy was performed on cultured PANC-1 cells. After serum starvation and stimulation with 100 ng/ml EGF for 1 h, cells expressing fluorescent protein–tagged versions of E-cad and Cav1 formed invaginations of the cell borders that contained both proteins. These Ecad/Cav1-containing invaginations were reminiscent of the "caveolar towers" seen at the ultra-

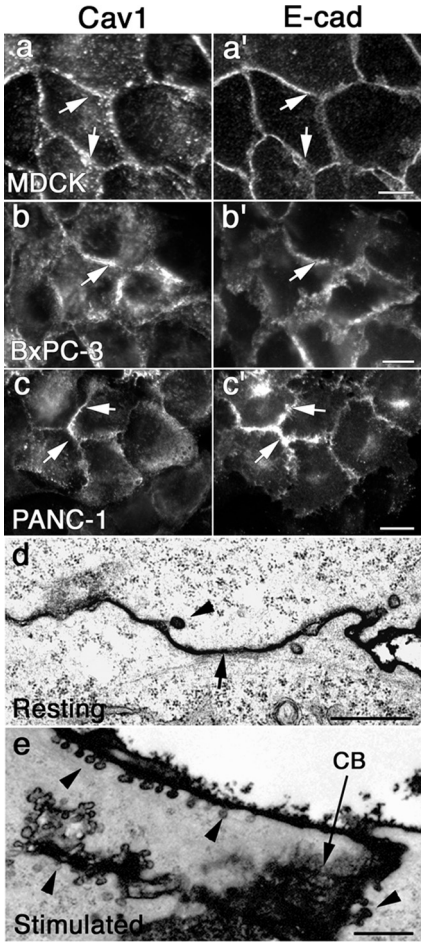

Figure 1. E-cad and Cav1 colocalize at sites of cell–cell contact in normal and pancreatic tumor epithelial cells before EGF stimulation. (a–c′) Fluorescence micrographs of normal MDCK cells (a and a′), the human pancreatic cancer cells BxPC-3 (b and b′), and PANC-1 (c and c′). All of the cell types display marked colocalization of endogenous Cav1 (a, b, and c) and E-cad (a′, b′, and c′) at the PM (arrows) under serum-starved conditions. (d) Electron micrograph of a region of cell–cell contact between two tightly apposed PANC-1 cells (arrow), demonstrating that relatively few caveolae (arrowhead) are present under serum-starved conditions. (e) Electron micrograph of PANC-1 cells stimulated with 30 ng/ml EGF for 20 min, showing a proliferation of individual caveolae and the formation of clustered "caveolar towers" (arrowheads) along an internalizing cell border (CB, arrow) of two adjacent cells. Scale bars, (a–c′) 10 μm; (d and e) 1 μm.

structural level After EGF treatment in these cells (Figure 1e, Orlichenko *et al.,* 2006). Short time-lapse observations revealed small vesicles carrying both E-cad and Cav1 proteins in the act of budding from these border invaginations toward the cell interior (Supplemental Figure S2 and Supplemental Movies 1 and 2). Interestingly, the Panc1 cell model utilized here facilitated this live time imaging as they possess tenuous, irregular cell borders with only modest peripheral E-cad that appears predominantly internalized within cytoplasmic vesicles. Thus, these cells appear to constitutively vesiculate and transport E-cad from the cell borders.

The dramatic formation of caveolae along with Cav1-coated, E-cad–containing vesicles in EGF-treated cells suggested that these conditions might induce an increased association between Cav1 and E-cad. First, to help discern whether the E-cad–containing endocytic structures actually represented endosomal compartments or rather clustered patches at the cell surface, 3D reconstruction of HPAF-II cells stimulated with EGF and stained for E-cad and Cav1 was performed. Indeed, as depicted by the representative 3D reconstruction in Supplemental Figure S3, most of the spherical Cav1- and E-cad–containing structures were within the central cytoplasm of each cell. Next, as EGF-induced phosphorylation of Cav1 might alter its interactions with proteins, we monitored Cav1 tyrosine 14 phosphorylation in MDCK and BxPC-3 cells treated with EGF by Western blot using an anti-phospho-Cav1 antibody (PY14). Both cell types showed a marked increase in Cav1 phosphorylation after EGF treatment, although significant levels of Cav1 were phosphorylated even under resting conditions in BxPC-3 cells (Figure 2c). This observation is consistent with the fact that these cells have amplified EGF receptor signaling (L.O., S.G.W., and M.A.M. unpublished observations; Arnoletti *et al.,* 2004; Ali *et al.,* 2005), modest cell–cell borders, and spontaneously form Cav1-coated endosomes in the absence of EGF treatment (Supplemental Figure S1, b and b′). Finally, to test for an association between Cav1 and E-cad and whether this putative interaction might be increased upon EGF stimulation, Cav1 was immunoprecipitated from MDCK and BxPC-3 cells at various time points after EGF stimulation. Subsequently, the immunoprecipitates were Western blotted for E-cad and phospho-Cav1, and the signal from the respective bands was quantitated using densitometry. Modest levels of E-cad were coimmunoprecipitated with Cav1 from both cell types in the absence of EGF; however, upon stimulation with EGF, a significant increase (twofold) in the amount of coimmunoprecipitated proteins was observed (Figure 2, d and e). Interestingly, this increase paralleled the observed increase in Cav1 phosphorylation in both cell types, with MDCK cells exhibiting a slower response (30–60 min) compared with BxPC-3 cells (5–20 min). Coimmunoprecipitation of E-cad and Cav1 may not represent a direct binding of these proteins, and we predict that these proteins are more likely to interact indirectly as part of a complex within an endocytic compartment. The fluorescence images (Figure 2, a–b‴, and Supplemental Figures S1 and S2) also suggest an indirect interaction, as the internalized E-cad cargo was not always observed to overlap with Cav1, but instead appeared to be surrounded by a Cav1-coated container.

Disrupting Caveolae Formation Results in a Stabilization of Cell Borders

We have recently shown that EGF-stimulation of cultured cells induces a four- to eightfold increase in caveolae-like structures at the cell surface as assessed by EM (Orlichenko *et al.,* 2006). These invaginations were confirmed as caveolae based on their size and shape, strong labeling with a Cav1 antibody by immuno-EM, sequestering of HRP-conjugated cholera toxin, and by immunofluorescent internalization of toxin. Importantly, expression of a Cav1 tyrosine phosphomutant Cav1Y14F, unable to be phosphorylated by Src at this residue, greatly reduces the formation of these invaginations along with a marked correlating decrease in toxin uptake. This mutant protein acts to inhibit caveolin assembly and provides a useful tool to test the role of caveolae in the internalization of cell borders. In addition, EGF-induced phosphorylation of Cav1 appears to strongly correlate with E-cad internalization and a marked increase in the association between Cav1 and E-cad (Figure 2 and Supplemental Figure S1). To expand on these findings, we tested whether expression of the Cav1Y14F mutant would prevent the internalization of E-cad from cell borders and thereby alter cell

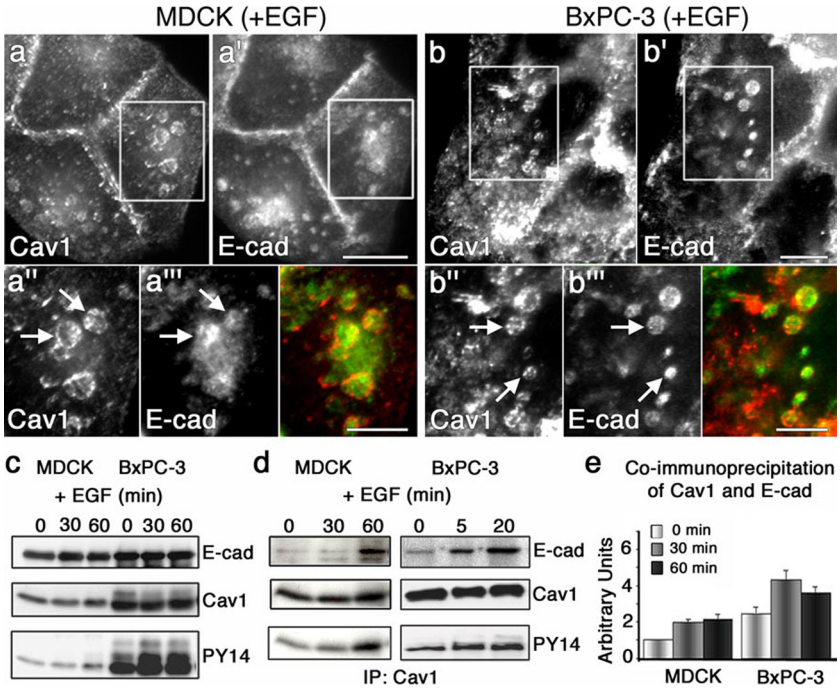

Figure 2. EGF stimulation of cultured cells promotes the internalization of E-cad into Cav1-coated endosomes. (a–b′) Fluorescence micrographs of MDCK (a and a′) and BxPC-3 cells (b and b′) treated with EGF for 20 min, showing the redistribution of Cav1 (a and b) and E-cad (a′ and b′) from the PM to intracellular locations. (a″, a‴, b″, and b‴) Higher magnification of the boxed regions in a and a′ and in b, b′, respectively, emphasizing the EGF-induced localization of Cav1 (a″ and b″) and E-cad (a‴ and b‴) to large, Cav1-coated endocytic structures (arrows). Merged images are shown in color. (c) Lysates from MDCK and BxPC-3 cells treated with EGF (100 ng/ml) for the indicated times were analyzed by Western blot using anti-E-cad, anti-Cav1, and anti-phospho-Cav1Y14 (PY14) antibodies. An increase in Cav1 phosphorylation at tyrosine 14 upon EGF treatment is observed in both MDCK and BxPC-3 cells; however, this phosphorylation is more prominent in the tumor cells. (d) Lysates from MDCK and BxPC-3 cells that were stimulated with EGF (100 ng/ml) for the indicated times were subjected to immunoprecipitation using an anti-Cav1 antibody, and the samples were subsequently analyzed by Western blot using antibodies against E-cad, Cav1, and phospho-Cav1Y14 (PY14). A marked increase in the association between E-cad and Cav1 is observed in both cell types after EGF stimulation, although this increased association occurs more rapidly in BxPC-3 cells. (e) Graph depicting results from densitometric quantitation of immunoprecipitation experiments similar to those shown in panel d (n = 3; results represent the average ± SEM). Scale bars, (a–b′) 5 μm; (a″–b‴) 2 μm.

morphology. Interestingly, MDCK cells stably expressing mRFP-tagged Cav1Y14F showed marked differences in cell–cell contacts, both at the light microscopy and EM levels. As shown in Figure 3, colonies of transfected MDCK cells could be identified using phase microscopy by appearance alone. Cells expressing Cav1Y14F-mRFP formed more tightly associated colonies than the surrounding untransfected cells, which appeared less organized. At the EM level, comparison of transverse sections of untransfected MDCK cells (Figure 3c) to MDCK cells stably expressing Cav1Y14F-mRFP (Figure 3, d and e) revealed a dramatic difference in the border morphology between the two cell populations.

Control cells displayed delicate, well-defined cell borders in close physical association with each other. In comparison, mutant cells possessed large, convoluted cell–cell borders that were three to four times the length of control cells. Observation of MDCK and BxPC-3 cells expressing mutant Cav1 using fluorescence microscopy (Figure 4, a–b′ and d–e′) also suggested that the cell–cell contacts were exceptionally large in these cells. Indeed, quantitation of E-cad fluorescence intensity indicated more than a twofold increase in E-cad at the cell borders of Cav1Y14F-mRFP–expressing cells compared with adjacent untransfected cells (Figure 4, c and f). These extensive E-cad–positive membrane domains observed by light microscopy apparently represent the excessively long borders protruding into the cell center that were so prominent in electron micrographs (Figure 3, d and e). To provide a biochemical method to measure E-cad clearance from the cell surface while further correlating caveolae assembly with cell junction internalization, we performed surface biotinylation experiments of cultured cells in the presence or absence of active src kinase. Because HPAF and BxPC-3 cells are very tightly associated making E-cad surface labeling difficult, we utilized MDCK cells. These particular cells have been engineered to stably express v-Src (activated at 35°C; Behrens *et al.*, 1993) and have been utilized by many others to study E-cad internalization (Fujita *et al.*, 2002) and cell dissemination during migration (Behrens *et al.*, 1993). We have previously utilized this cell model to demonstrate Src-induced caveolin assembly at cell borders (Orlichenko *et al.*, 2006). In this current study, cells stably expressing either Wt Cav1 or mutant CavY14F were shifted to the permissive temperature for 7 h before surface biotinylation to label all surface proteins. E-cad protein was then immunoprecipitated from cells, run on SDS-PAGE and probed with streptavidin-conjugated HRP. Quantitation of three separate experiments showed a significant reduction in E-cad internalization in the CavY14F mutant expressing cells compared with that of the Wt Cav1-expressing cells (Figure 4, g and h), consistent with the morphological measurements (Figure 4c).

Caveolae have been linked to regulation of a variety of different cell signaling cascades including Src and Erk kinase as well as rac (Engelman *et al.*, 1998; Grande-Garcia *et al.*, 2007; Patel *et al.*, 2008). Altered activity of these pathways by manipulation of caveolin could alter cell–cell contacts indirectly rather than by caveolae formation. To address this, we assessed active levels of phosphorylated forms of Src and ERK in cells expressing either Wt-Cav1-GFP or CavY14F-GFP proteins. We viewed this approach as preferable to a Cav1 siRNA knockdown approach that would decrease the levels of Cav1 protein. Instead, all cells examined would express equal levels of Cav1, with the only difference being a change in a single tyrosine substitution that alters caveolae assembly. HPAF cells expressing either GFP-tagged wt or mutant Cav1 were stimulated with EGF for 15 min and then lysed and blotted for phospho-active forms of C-Src or Erk kinases. As shown in Supplemental Figure S4, we observed no appreciable change in the levels of these activated kinases, suggesting that changes in E-cad internalization were not due to altered signaling cascades. In addition, as shown later, we have conducted cell separation/dissemination studies with these caveolin mutant proteins.

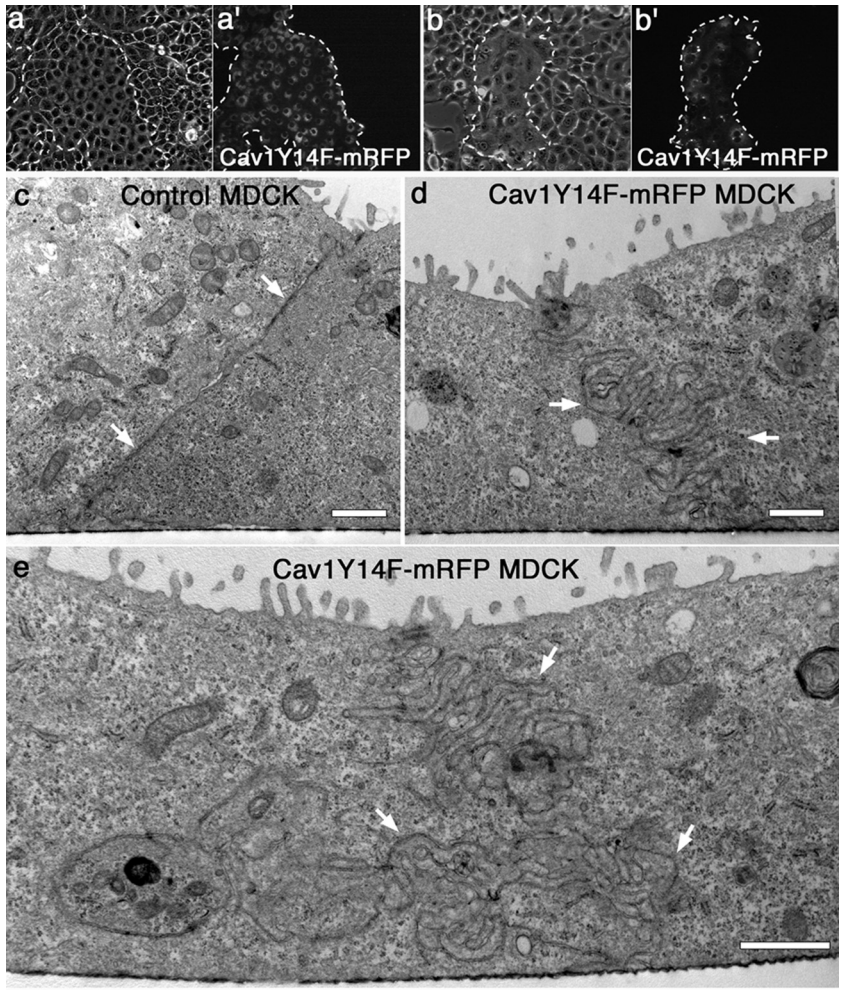

Figure 3. Preventing caveolae assembly through expression of a phospho-mutant Cav1 (Cav1Y14F-mRFP) induces marked changes in the morphology of cell colonies and cell–cell contacts. (a–b′) Corresponding phase (a and b) and fluorescence (a′ and b′) micrographs of mixed populations of parental untransfected MDCK cells and MDCK cells stably expressing mRFP-tagged Cav1Y14F. The two populations of cells exhibit noticeable differences in cell–cell attachment, spreading, and general morphology, allowing them to be distinguished from one another even by phase microscopy at low levels of magnification. Dashed lines provide fiduciary marks surrounding the colonies of transfected cells. (c–e) Electron micrographs of parental untransfected MDCK cells (c) and MDCK cells stably expressing Cav1Y14F-mRFP (d and e). When sectioned in the transverse orientation, the junctions between the parental untransfected cells appear thin and easy to resolve (c, arrows). In contrast, the Cav1Y14F-mRFP-expressing cells display convoluted cell borders of exceptional length (d and e; arrows) that extend inward toward the cell center. Further, these borders are remarkably thick, consistent with fluorescence micrographs of the E-cad staining in cells expressing Cav1Y14F-mRFP (Figure 4). Scale bars, (c–e) 1 μm.

Because the morphology of cell borders in Cav1Y14F-expressing cells was markedly different at the light and ultrastructural levels, we next tested whether these differences translated into functional alterations at cell–cell contacts. This was done in three ways: first, by comparing the membrane dynamics at cell borders of living HPAF-II cells stably expressing wt Cav1-GFP versus the tyrosine phospho-mutant Cav1Y14F-GFP using time-lapse fluorescence microscopy (Figure 5, a–c); second, by measuring the TER exhibited by confluent monolayers of untransfected MDCK cells or MDCK cells stably expressing GFP alone, wt Cav1-GFP or Cav1Y14F-mRFP (Figure 5d); and third, by measuring cell dissemination. With live cell imaging, cells expressing Cav1-GFP were observed to display very dynamic borders, undergoing extensive membrane protrusions and retractions and at times appearing to separate (Figure 5, a and b). Most remarkable was the frequent formation of Cav1-GFP–coated membrane tubules and vesicles that extended rapidly from the cell borders, reflecting the internalization process viewed in fixed cells by EM (Figure 1e) and fluorescence microscopy (Figure 2, a–b‴). In marked contrast, HPAF-II cells expressing Cav1Y14F-GFP possessed static, well-defined borders that were lined with substantial amounts of Cav1Y14F-GFP, which remained relatively stable even after EGF stimulation (Figure 5c). A colocalization between Cav1 and endogenous E-cad at surface invaginations is more evident in fixed cells expressing the Cav1Y14F mutant protein (Figure 5, e–e″) consistent with the premise that caveolae formation is required for this internalization process. In addition, TER was increased two- to threefold as early as 24 h after confluency in MDCK cells stably expressing Cav1Y14F-mRFP compared with untransfected cells or cells expressing GFP or Cav1-GFP (Figure 5d).

As an alternative to overexpression of mutant Cav1, we next tested the effects of altering Cav1 function in MDCK and BxPC-3 cells using an approach that would not require exogenous protein expression. Namely, siRNA technology was used to reduce Cav1 expression levels, and the effects on E-cad localization at cell borders was assessed, we predicted that interfering with caveolae formation through reduction of Cav1 protein levels would also prevent caveolae-based internalization of AJ proteins, thus leaving more E-cad at the cell surface than in control cells, which was similar to cells expressing mutant Cav1. We and others have previously confirmed that treatment of cultured cells with the siRNA sequence used to target human Cav1 substantially reduces Cav1 protein levels, as assessed by Western blot analysis (Cho *et al.*, 2003; Orth *et al.*, 2006). MDCK and BxPC-3 cells were either mock-treated, as a control, or treated with Cav1 siRNA for 48 (MDCK) and 72 (BxPC-3) h and then fixed and stained with antibodies against Cav1 and E-cad. Images from control and Cav1 knockdown cells were acquired and adjusted in an identical way. As shown in Figure 6, in comparison to mock-treated cells (Figure 6, a, a′ and d, d′), cells treated with Cav1 siRNA (Figure 6, b, b′ and e, e′) exhibited markedly more (up to 2.5-fold) E-cad at their

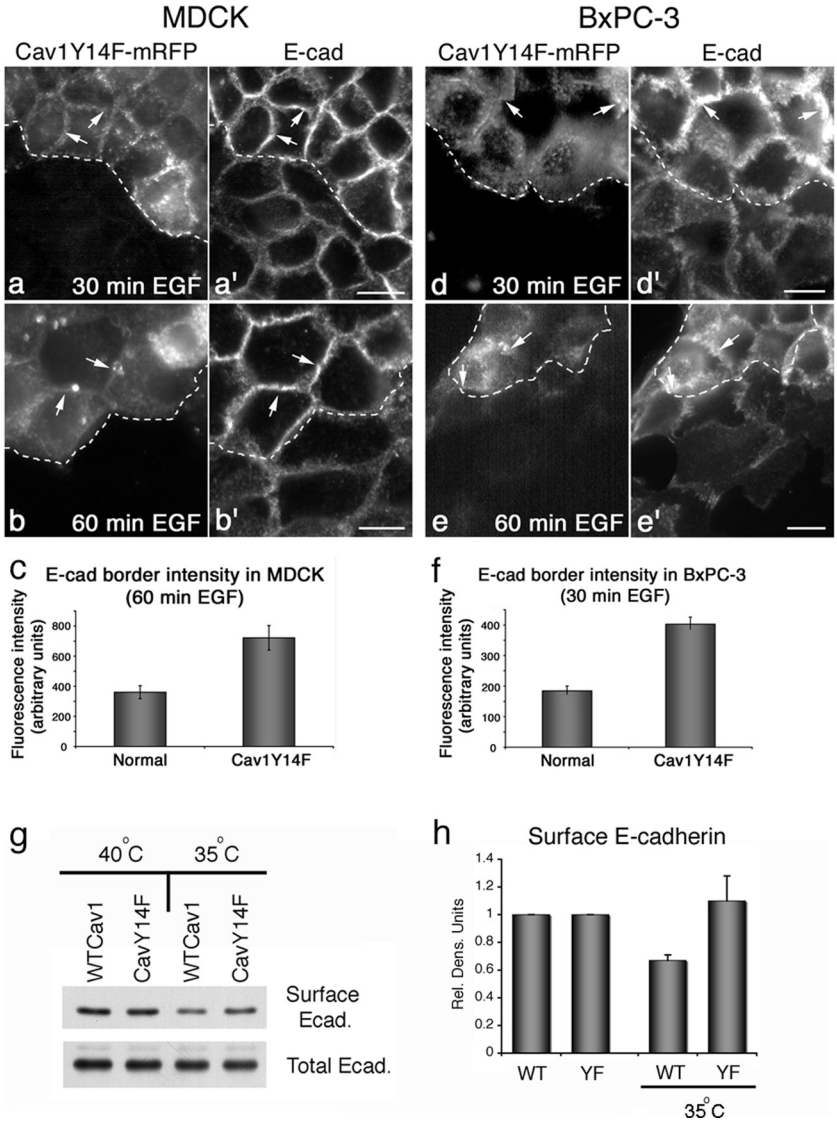

Figure 4. EGF-stimulated internalization of E-cad is reduced in both normal and neoplastic cells expressing the Cav1 tyrosine phospho-mutant Cav1Y14F. (a–b′ and d–e′) Fluorescence micrographs of mixed populations of parental untransfected cells and cells stably expressing mRFP-tagged Cav1Y14F (a, b and d, e) that were fixed and stained for E-cad (a′, b′ and d′, e′) after EGF stimulation (30 ng/ml) for the indicated times. Markedly increased levels of E-cad are present at the cell borders of Cav1Y14F-mRFP–expressing cells (arrows), compared with the modestly stained untransfected adjacent cells. Fluorescence micrographs of MDCK cells are shown in (a–b′) and of BxPC-3 cells in (d–e′). Dashed white lines provide fiduciary marks indicating the interface between transfected and untransfected cells. (c and f) Graphs depicting results of fluorescence quantitation of E-cad levels at cell borders. E-cad levels at the borders of Cav1Y14F-mRFP–expressing cells are increased two- to threefold compared with untransfected cells. Results represent the average ± SEM for ≥15 cells for each condition. (g) Western blot analysis of MDCK cells stably expressing a temperature-sensitive version of v-Src that were also transiently expressing either WTCav1 or Cav1Y14F. E-cadherin protein was immunoprecipitated from cells after surface biotinylation after a permissive temperature shift to activate v-Src at 35°C for 7 h. Surface E-cadherin was detected using streptavidin-conjugated HRP. (h) Graph showing the relative level of surface E-cadherin after a 7-h permissive temperature shift in cells expressing either WTCav1 or the Cav1Y14F mutant. Cells expressing the Cav1Y14F protein do not internalize surface E-cad, whereas the wt-expressing cells had a 40% reduction in surface protein after v-Src activation. Data represent the average level of surface E-cadherin normalized to total immunoprecipitated protein over three separate experiments. Error bars, SEM. Scale bars, (a–b′ and d–e′) 10 μm.

borders. In some instances, the borders of siRNA-treated cells were so enlarged that they appeared to form large sheets of E-cad that extended into the cytoplasm. (Figure 6, b′, c, e′, and f). As the siRNA probe was made to human Cav1, we observed a more efficacious reduction of Cav1 in the human cancer cells than in the canine MDCK cells, and this difference was also reflected by the substantial increase in E-cad at the cell borders of siRNA-treated BxPC-3 cells compared with the significant but more modest increase observed in MDCK cells (Figure 6, graphs). Regardless of the cell type used, these findings support the premise that a decrease in Cav1 protein, and thus caveolae, translates into greater levels of E-cad at cell borders.

Pancreatic Tumor Cells with Abnormal Cell–Cell Adhesions Exhibit Spontaneously Altered Cav1 Levels

The pancreatic tumor cell lines examined in this study exhibit markedly distinct degrees of cell–cell adhesion; therefore, we next tested whether these differences in morphological phenotypes might correlate with the endogenous protein levels of Cav1 and E-cad. Western blot analysis indicated that BxPC-3 cells express equal levels of Cav1 and E-cad protein (data not shown), similar to that observed in MDCK cells, while PANC-1 cells express modest E-cad protein levels, but normal levels of Cav1 protein (Figure 7a; see also Lin *et al.*, 2005), corresponding with the weak cell–cell interactions displayed by these cells. Similarly, staining of these cells using immunofluorescence showed that many of these loosely associated cells express robust levels of Cav1, but little E-cad protein (Figure 7, b and b′). Interestingly, small populations of PANC-1 cells do interact to form semi-tight monolayers and stain positive for E-cad (see also Furuyama *et al.*, 2000), but express very little Cav1 protein. Thus, this cell line displays an inverse correlation between Cav1 and E-cad protein expression, consistent with the prediction that cells without Cav1 protein cannot form caveolae and therefore E-cad levels at the cell borders remain high.

Examination of HPAF-II pancreatic tumor cells both by Western blot and immunofluorescence provided further support to the concept that an inverse correlation in Cav1 and E-cad protein levels translates to effects on AJ integrity. Compared with the other normal and neoplastic cells examined in this study, HPAF-II cells express exceptionally high levels of E-cad protein and very little (10%) Cav1 (Figure 7a;

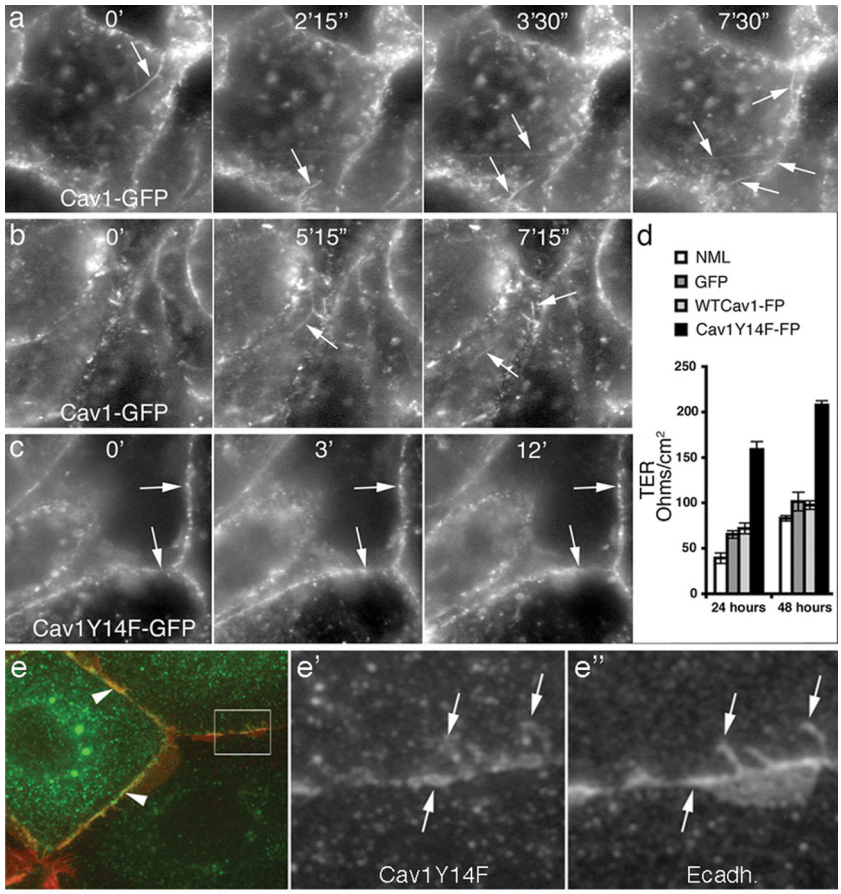

Figure 5. Cells expressing the Cav1 tyrosine phospho-mutant Cav1Y14F exhibit reduced border dynamics as well as an increase in transepithelial electrical resistance. (a–c) Select still fluorescence images from movies of HPAF-II cells stably expressing wt Cav1-GFP (a and b) or the Cav1 tyrosine phospho-mutant Cav1Y14F-GFP (c). Imaging was initiated approximately 5 min after the addition of EGF (30 ng/ml); time frames (minutes and seconds) are indicated at the top of each image. Cells expressing wt Cav1-GFP exhibit very dynamic borders from which many Cav1-coated vesicles and tubules are liberated (a and b; arrows). In contrast, cells expressing Cav1Y14F-GFP display static, linear borders (c; arrows) that exhibit little membrane dynamics. (d) Graph depicting the transepithelial electrical resistance (TER) of normal, untransfected (NML) MDCK cells, control MDCK cells stably expressing GFP, MDCK cells stably expressing GFP-tagged wt Cav1 (WTCav1-FP), and MDCK cells stably expressing mRFP-tagged Cav1Y14F (Cav1Y14F-FP). Measurements were taken 24 and 48 h after cells had reached confluency. Cells expressing Cav1Y14F-mRFP showed a two- to threefold increase in TER, compared with untransfected MDCK cells or cells stably expressing GFP alone or GFP-tagged wt Cav1 (n = 3; results represent the average ± SD). (e–e″) To look for colocalization of E-cad in Cav1-coated membrane invaginations, cells expressing wt or mutant Cav1Y14F were fixed and stained for both proteins. Cav1-positive punctate protrusions of the cell membrane were observed to be markedly positive for E-cad, particularly in cells expressing the mutant Cav1Y14F protein. Scale bars, 10 μm.

see also Rajasekaran *et al.*, 2004; Lin *et al.*, 2005). These cells form remarkably strong AJs, because they assemble into tight colonies that cannot be dissociated during passage unless exceptionally high concentrations of trypsin are combined with prolonged incubations. Additionally, these cells do not disseminate upon treatment with high serum or EGF stimulation. Immunofluorescence analysis confirmed that very high levels of E-cad are present at the borders of HPAF-II cells, and further, these cells form unusually developed AJs that are so extensive as to extend into the central cytoplasm (Figure 7c; see also Rajasekaran *et al.*, 2004). Importantly, this unique staining pattern was not observed in any other cell type we have examined, except those treated with siRNA to reduce cellular Cav1 levels. Thus, as for the PANC-1 cells, there is also a strong inverse correlation between Cav1 and E-cad protein levels in HPAF-II cells.

The spontaneously low levels of Cav1 protein exhibited by the HPAF-II tumor cells could be a bona fide cause for the very high E-cad levels and unusually strong cell–cell contacts demonstrated by these cells. Therefore, we tested whether artificially elevating levels of Cav1 protein through exogenous expression of wt Cav1-GFP might compromise the markedly adherent phenotype exhibited by these cells as well as increase their propensity to disseminate after EGF treatment by facilitating E-cad internalization. This was tested using a variety of different approaches to look for a confirming trend. First, cells were microinjected (Figure 7, d–e′) or transfected with constructs encoding Cav1-GFP or GFP, as a control, and allowed to recover (12 h). Subsequently, colonies of HPAF-II cells were serum-starved overnight and then stimulated with 30 ng/ml EGF for 16–24 h before fixation and staining for E-cad. Cells were counted as disseminated if three of four borders were no longer in contact with adjacent cells. Although ~26% of the Cav1-GFP–expressing HPAF-II cells acquired a motile phenotype and disseminated outward from the tightly associated colonies (Figure 7, d′ and e′), only 12% of the cells expressing the Cav1Y14F mutant exhibited a dissemination response to EGF. Further, HPAF-II cells expressing Cav1-GFP could be easily identified not only by the Cav1-GFP (Figure 7, d′ and e′), but also by the dramatic reduction of E-cad staining in the cytoplasm and at the cell borders. Indeed, compared with the surrounding untransfected cells, Cav1-GFP–expressing HPAF-II cells had little, if any, E-cad at the cell borders. In support of the experiments using a CavY-14F mutant protein to prevent caveolae assembly, a phosphomimetic form (Cav1Y14D), was utilized to accentuate assembly to test if this might increase cell separation. This mutant has been utilized by others and demonstrated to increase the internalization of cell adhesions (Joshi *et al.*, 2008) and also increase cholesterol transport from the cell surface (Caldieri *et al.*, 2008).

We have provided additional characterization of this mutant protein through expression in NRK cells and measuring the effects on caveolae formation by ultrastructural examination. As displayed in Supplemental Figure S5, EM of nontransfected control NRK cells show normal numbers of caveolae (0.8/10 μm of PM), whereas those expressing the Cav1Y14F mutant assemble markedly less (0.58/10 μm of PM). These findings are consistent with our original findings (Orlichenko *et al.*, 2006). In contrast, cells expressing the wt Cav1 or the Cav1Y14D mutant assemble many more caveo-

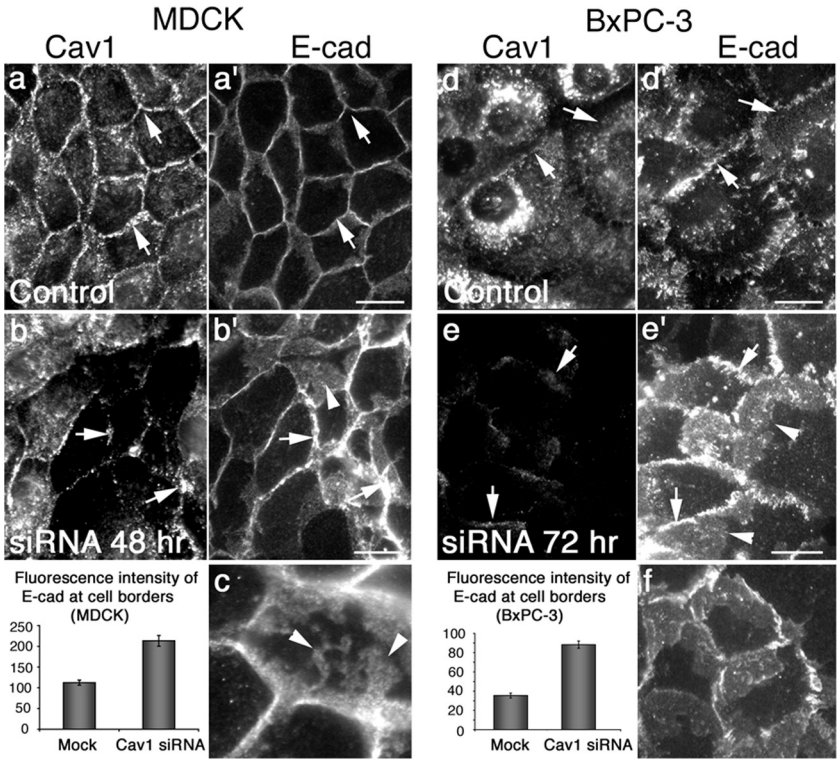

Figure 6. SiRNA-mediated knockdown of Cav1 increases the levels of E-cad at cell borders. (a, a′ and d, d′) Fluorescence micrographs of MDCK (a and a′) and BxPC-3 cells (d and d′) stained for Cav1 (a and d) and E-cad (a′ and d′) under normal growth conditions, indicating the basal levels of E-cad present at cell borders (arrows). (b, b′ and e, e′**)** MDCK cells (b, b′) and BxPC-3 cells (e, e′) treated with Cav1 siRNA for 48 and 72 h, respectively, showing a decreased level of Cav1 (b and e, arrows) and corresponding increase in E-cad levels at cell borders (b′ and e′, arrows). (c and f) Higher magnification images focused on E-cad distribution at the cell borders of siRNA-treated MDCK (c) and BxPC-3 (f) cells. Abnormally high levels of E-cad accumulate at cell borders in these cells, reflecting a lack of border internalization and resulting in the formation of robust junctions that appear to extend large laminar protrusions into the central cytoplasm (arrowheads). Graphs depict results from fluorescence quantitation of E-cad levels at cell borders in mock-treated and Cav1 siRNA-treated cells. Reduction of Cav1 levels results in a 2- to 2.5-fold increase in E-cad levels at cell borders. Results represent the average ± SEM for >15 cells for each condition. Scale bars, (a–b′ and d–e′) 10 μm.

lae (1.3/10 μm of PM and 1.06/10 μm of PM). Importantly, the caveolae in the Y14D-expressing cells appear more clustered and distal to the PM, as if internalized, compared with the control or wt–expressing cells. Although we cannot make firm conclusions on caveolae association with the PM without ruthenium red EM approaches, these findings do support the concept that increased phospho-Cav1 protein sustain the internalization of E-cad vesicles into the cell interior. Indeed, we observed a considerable number (35%) of the large caveosome-like, E-cad–associated structures in the CavY14D expressing cells compared with controls (Supplemental Figure S5). Thus, cells expressing the phosphomimetic form of Cav1 form markedly more caveolae than control cells or cells expressing Cav1Y14F, are more effective in the internalization of cell adhesions (Joshi *et al.*, 2008) and surface cholesterol (Caldieri *et al., 2008*) and form large E-cad containing caveosomes.

After the characterization of the Cav1 phosphomimetic–expressing cells we tested if this might support or accentuate tumor cell dissemination. Cells expressing this Cav1Y14D protein also internalized borders and moved away from adjacent untransfected cells (Figure 7f). Interestingly, these migratory mutant Cav1-expressing cells often left a distal appendage, revealing its original attachment site within the colony before transfection. As a third approach, HPAF cells expressing either wt or mutant Cav1 were cotransfected with an active form of Src kinase (c-Src Y530F) to further potentiate any observed effects of Cav1 expression on cell–cell contacts. A stable cell line of Cav1-expressing HPAF cells were utilized, as were transiently transfected cells (Figure 7g). We observed a near twofold increase in dissemination rates of the Cav1 wt stable-expressing cells compared with the Cav1Y14F mutant, whereas the effect observed in the transiently transfected cells was even more dramatic (six- to sevenfold increase of Cav1 wt, Cav1Y14D vs. Cav1Y14F). These "rescue" experiments provide graphic support indicating an important role for caveolae in the localization and internalization of E-cad in these pancreatic tumor cells. Finally, to confirm the effect of the Cav1Y14D-GFP on cell dissemination and morphology, MDCK cells were transiently transfected to express this protein then were fixed and stained for E-cad after a 48-h incubation. As the MDCK cells do not express high levels of Src or EGFR like the PANC1 cells, we expected that the effect of the phospho-mimetic Cav1 form to be accentuated in this cell type. Indeed, transfected cells exhibited a dispersed phenotype leaving long vestigial appendages as the HPAF cells (Figure 7h, arrow) but exhibited a six- to sevenfold increase in dissemination compared with wt-expressing cells.

DISCUSSION

In this study we have made several important observations implicating both caveolae and Cav1 in the EGF-stimulated internalization of the AJ protein E-cad in both normal epithelial cells and human pancreatic ductular tumor cells. We find that Cav1 and E-cad colocalize at cell junctions in resting cells, and furthermore, that as the epithelial cells begin to separate after treatment with EGF, E-cad is internalized into numerous endocytic structures coated with Cav1 (Figure 2, a–b‴ and Supplemental Figures S1 and S2). Concomitant with this vesiculation is an increased association between Cav1 and E-cad (Figure 2, d and e). Src-mediated phosphorylation of Cav1 occurs at tyrosine 14 (Li *et al.*, 1996; Lee *et al.*, 2000) and is induced upon treatment of MDCK and BxPC-3 cells with EGF (Figure 2c). Interestingly, we observed that expression of the tyrosine phospho-mutant Cav1Y14F prevents caveolae formation in these cells as well as induces a marked change in cell morphology, a remarkable increase in the complexity of the adhesion sites between adjacent cells, and an accumulation of E-cad at cell–cell contacts (Figures 3 and 4). In support of these findings, living cells stably ex-

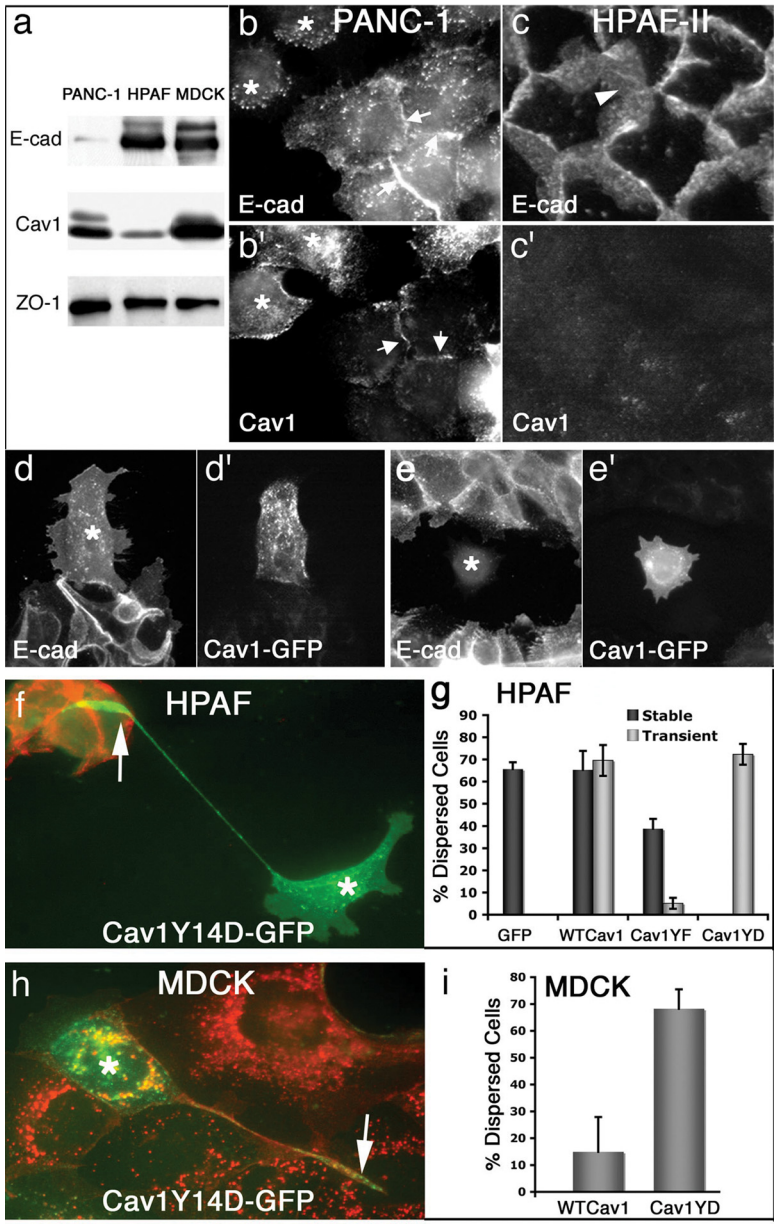

Figure 7. Pancreatic tumor cells display differences in endogenous levels of Cav1 protein that inversely correlate with the integrity of E-cad–based cell–cell contacts. (a) Lysates from PANC-1 and HPAF-II cells, two pancreatic tumor cell types, and MDCK cells were analyzed by Western blot using antibodies against E-cad, Cav1, and the junctional protein ZO-1 (as a loading control). Note the inverse correlation between endogenous levels of E-cad and Cav1 in both tumor cell types, compared with the MDCK cells. (b–c′) Fluorescence micrographs of PANC-1 (b and b′) and HPAF-II (c and c′) cells stained for E-cad (b and c) and Cav1 (b′ and c′) also indicate this inverse correlation while additionally showing the effects on cell–cell adhesion. PANC-1 cells exist as a heterogeneous population, and indeed, dispersed cells appear to have little E-cad at the borders (b, *) with normal Cav1 (b′) levels, whereas cells associated in a cluster have E-cad at their borders, but show very little Cav1 staining (arrows). HPAF-II cells are more homogeneous and possess remarkably strong interactions, with substantial levels of E-cad (c, arrowhead) present at the borders, whereas Cav1 (c′) staining is modest. (d–e′) Fluorescence micrographs of HPAF-II cells microinjected with a construct encoding for Cav1-GFP that were allowed to recover from microinjection then serum-starved, treated for 24 h with 30 ng/ml EGF, fixed, and stained for E-cad. Microinjected cells (*) expressing Cav1-GFP (d′ and e′) display little E-cad (d and e) and have a higher propensity to break away from the tightly associated cell colonies and move outward. (f) An HPAF-II cell (*) expressing a phospho-mimetic Cav1Y14D-GFP after conventional transfection that can be seen migrating away from adjacent, tightly clustered, nontransfected cells leaving a remnant appendage of its original location (arrow). Note the high levels of E-cad in the untransfected cells (red), whereas the disseminated cell has no E-cad. (g) HPAF-II cells stably or transiently expressing either WTCav1-GFP or Cav1Y14F-GFP have different migratory behaviors when subjected to active Src coexpression. Quantitation of dissemination by HPAF cells expressing different forms of exogenous Cav1 protein. The majority of cells (>60%) expressing either GFP, WTCav1GFP, or Cav1Y14D were separated or detached from neighboring cells, whereas cells expressing Cav1Y14F-GFP were less migratory. Only 39% of the cells stably expressing CavY14F and 5% of the HPAF cells transiently expressing this mutant CavY14F protein displayed a disseminated phenotype. Data are the average of three experiments for the stable lines and two experiments for the transient transfections. Error bars, SEM. (h) A single MDCK cell transfected (*) to express Cav1Y14F-GFP has migrated away from its original attachment site (arrow) to the periphery of the colony of untransfected cells. (i) Quantitation of transfected MDCK cells that have dispersed away from adjacent cells. Importantly, cells expressing the Cav1Y14D protein display a six- to sevenfold increase compared with wt-expressing cells.

pressing this mutant Cav1 showed markedly less membrane dynamics at cell borders when imaged using time-lapse microscopy and over a twofold increase in TER (Figure 5). Similarly, reduction of Cav1 protein levels by siRNA treatment also led to an increase in E-cad at the borders of EGF-stimulated cells (Figure 6). Finally, we found that an inverse correlation between Cav1 levels and cell–cell adhesion exists in several pancreatic tumor cell types. Most remarkably, HPAF-II cells, which normally form very adherent colonies of cells and express exceedingly low levels of Cav1, could be induced to disseminate from the cell colony if transfected with a construct allowing for exogenous expression of Cav1. To our knowledge these findings provide the first demonstration that directly preventing caveolae assembly, through either expression of a mutant Cav1 or siRNA-mediated knockdown of Cav1, not only decreases the internalization of E-cad, but also leads to a marked proliferation of cell–cell contacts.

EGF-induced Internalization of Adherens Junction Proteins into Caveolin-coated Endosomes

Although there has been substantial interest in the potential role of caveolae as a mechanism for internalizing components of cell junctions, there have been few, if any, studies that have actually conducted a comparative analysis of this process using both EM and light microscopy. The conspicuous formation of E-cad–containing, Cav1-coated endosomes correlated temporally with an increased association between these proteins observed by biochemical methods (Figure 2). Currently it is not known whether this interaction

represents a direct binding of E-cad to Cav1 or rather an association of these two proteins as part of a multiprotein complex. Although we observed the formation of Cav1-coated endosomes filled with E-cad in all four types of cells tested in this study, it is important to note that only the non-neoplastic MDCK cells required stimulation with EGF to form these organelles. In contrast, the pancreatic tumor cells appeared to cointernalize E-cad and Cav1 spontaneously, although this could be increased by EGF stimulation. This is consistent with observations that MDCK cells require activation of Src, such as through expression of v-Src or after growth factor stimulation, to disassemble cell borders before separation (Palacios *et al.*, 2001, 2005; Orlichenko *et al.*, 2006), whereas PANC-1 and BxPC-3 cells exhibit weak junctions, form modest monolayers, and have elevated signaling cascades as part of the neoplastic condition (L.O., S.G.W., and M.A.M. unpublished observations; Korc *et al.*, 1986; Arnoletti *et al.*, 2004; Ali *et al.*, 2005). Thus, these cells may exhibit a more dynamic turnover of E-cad, contributing to a more constitutive formation of Cav1-coated, E-cad–containing endosomes as well as the malignant phenotype.

Cell–Cell Contacts Are Robust in Cells with Compromised Caveolae Function

Our findings are consistent with the premise that epithelial cells use caveolae to internalize E-cad and disassemble cell junctions in response to EGF stimulation. Of equal importance is the inverse finding that inhibiting the assembly of caveolae through siRNA-mediated reduction of Cav1 levels or expression of the Cav1Y14F mutant results in an accumulation of E-cad at cell borders, altered cell morphology, and an extensive elaboration of cell–cell contacts. These findings are intriguing as they both support and contrast with a study where E-cad internalization after treatment with EGF was analyzed in A431 cells, an epidermoid carcinoma cell line. Similar to our studies, acute treatment of A431 cells with EGF induced E-cad internalization and disruption of cell–cell junctions. Furthermore, the EGF-stimulated internalization of E-cad could be attenuated by cholesterol-depleting drugs that interfere with caveolae assembly (Lu *et al.*, 2003). However, prolonged EGF treatment of A431 cells led to a decrease in both Cav1 and E-cad expression at the transcriptional level and a subsequent enhancement in cell invasion. In addition, reduction of Cav1 levels through an expression of antisense Cav1 RNA also resulted in decreased expression of E-cad and an enhancement in cell invasion. Possibly these distinct observations are due to differences in the cell types studied. We did not analyze Cav1 and E-cad localization or protein levels after treatment of cells for prolonged time periods with EGF. Thus, our current study does not implicate transcriptional regulation, possibly a more downstream effect, but instead provides evidence that under conditions of acute EGF treatment, caveolae serve as an endocytic mechanism for the internalization of AJ proteins. The fact that we observed similar cellular responses—an increase in the size of cell–cell contacts, an accumulation of border-localized E-cad, and an increase in TER—upon expression of a mutant Cav1 (Cav1Y14F) or reduction in endogenous Cav1 protein via siRNA treatment seems relevant and important. Moreover, these findings are consistent with the observations made in the pancreatic tumor cells regarding expression levels of Cav1 and E-cad and AJ integrity.

In the cell models used for our study, we observed an inverse correlation between Cav1 and E-cad protein levels under a variety of experimental conditions. Using fluorescence microscopy, we observed that siRNA-mediated reduction of Cav1 protein levels leads to a marked (two- to three-fold) increase in E-cad at the cell borders both in MDCK and BxPC-3 cells, compared with untreated cells. In this case, quantitative analysis was performed using imaging software to measure the fluorescence intensity of E-cad at the cell borders only, not accounting for total cellular E-cad. Perhaps most compelling is the spontaneous inverse correlation of E-cad and Cav1 levels in two of the pancreatic tumor cell types studied here. Western blot analysis of total cell lysates from PANC-1 cells indicated that these cells express relatively normal levels of Cav1 (see also Lin *et al.*, 2005), compared with MDCK cells, yet more modest E-cad levels. Interestingly, immunofluorescence analysis revealed that these cells appear to grow as two populations with distinct morphologies: one population forms modest junctions that stain for E-cad but contain little Cav1, whereas the second population of cells are generally completely dissociated from each other and express higher levels of Cav1, but reduced levels of E-cad (see also Furuyama *et al.*, 2000). In contrast to the distinct populations of PANC-1 cells, HPAF-II cells form exceptionally tight monolayers. Furthermore, supportive of the inverse correlation observed in PANC-1 cells but even more graphic in nature, HPAF-II cells express little Cav1 (see also Lin *et al.*, 2005), as assessed by Western blot analysis, but relatively high amounts of E-cad (see also Rajasekaran *et al.*, 2004). Thus, the phenotypes observed in the specific cell types studied here with reduced expression levels of Cav1, either through experimental manipulation (siRNA treatment) or simply as a result of endogenous regulation, are consistent with the concept that a reduction in Cav1 levels and/or caveolae function potentiates E-cad–based cell–cell adhesion.

Caveolae Function in Pancreatic Tumor Cell Dissemination and Invasion

The multiple experimental approaches used in this study suggest that Cav1/caveolae play a central role in facilitating the dissociation of pancreatic tumor cells, and potentially other epithelial-based tumors, with activated signaling cascades. Currently the literature implicating caveolin levels in neoplasia is extensive but also complex (for recent reviews see Goetz *et al.*, 2008; Tanase, 2008). For example, several studies have shown a correlation between a decrease in Cav1 expression leading to an acceleration in the development of mammary lesions, tumorigenesis, and invasiveness (Williams *et al.*, 2003, 2004). In addition, normal Cav1 levels have been implicated in down-regulating RhoC GTPase and thereby attenuating migration and invasion of pancreatic tumor cells (Lin *et al.*, 2005). In contrast, increased Cav1 levels have been implicated in promoting prostate tumor progression (Williams and Lisanti, 2005), whereas increased Cav1 levels have also been implicated in breast tumors (Van den Eynden *et al.*, 2006) and pancreatic adenocarcinoma (Suzuoki *et al.*, 2002).

A contribution made by our current study is a mechanistic connection between Cav1 protein and the formation/assembly of caveolae vesicles that leads to tumor cell dissemination. Certainly there are other cellular processes that could contribute to this dispersal process in addition to caveolae formation. However, the studies indicating an increase in the ability of HPAF-II cells to disseminate when exogenously expressing wt Cav1 protein (Figure 7) are particularly compelling, because these cells express little endogenous Cav1 and form remarkably adherent colonies. Furthermore, they are consistent with recent publications implicating Cav1 and caveolae formation in cell migration (Navarro *et al.*, 2004; Grande-Garcia *et al.*, 2007). Thus, although caveolae have been implicated in both facilitating and attenuating cell mi-

gration (Navarro *et al.*, 2004; Lin *et al.*, 2005), our findings suggest a potential positive role for caveolae in mediating the dissemination process in some types of pancreatic tumor cells through their effects on the disassembly of AJs and subsequent cell separation. As such, interfering with caveolae or Cav1 function could represent a therapeutic target in an effort to help prevent or control the metastasis of some tumors (van Golen, 2006).

ACKNOWLEDGMENTS

The authors thank Dr. H. M. Thompson (Mayo Clinic) for help in preparing the manuscript. This work was supported by National Institutes of Health/National Cancer Institute Grant CA 104125 (M.A.M.) and the Optical Morphology Core of NIHDK 84567.

REFERENCES

Ali, S., El-Rayes, B. F., Sarkar, F. H., and Philip, P. A. (2005). Simultaneous targeting of the epidermal growth factor receptor and cyclooxygenase-2 pathways for pancreatic cancer therapy. Mol. Cancer Ther. *4*, 1943–1951.

Alldinger, I., *et al.* (2005). Gene expression analysis of pancreatic cell lines reveals genes overexpressed in pancreatic cancer. Pancreatology *5*, 370–379.

Arnoletti, J. P., Buchsbaum, D. J., Huang, Z. Q., Hawkins, A. E., Khazaeli, M. B., Kraus, M. H., and Vickers, S. M. (2004). Mechanisms of resistance to Erbitux (anti-epidermal growth factor receptor) combination therapy in pancreatic adenocarcinoma cells. J. Gastrointest. Surg. *8*, 960–969.

Behrens, J., Vakaet, L., Friis, R., Winterhager, E., Van Roy, F., Mareel, M. M., and Birchmeier, W. (1993). Loss of epithelial differentiation and gain of invasiveness correlates with tyrosine phosphorylation of the E-cadherin/beta-catenin complex in cells transformed with a temperature-sensitive v-SRC gene. J. Cell Biol. *120*, 757–766.

Bryant, D. M., and Stow, J. L. (2004). The ins and outs of E-cadherin trafficking. Trends Cell Biol. *14*, 427–434.

Caldieri, G., Giacchetti, G., Beznoussenko, G., Attanasio, F., Ayala, I., and Buccione, R. (2008). Invadopodia biogenesis is regulated by caveolin-mediated modulation of membrane cholesterol levels. J. Cell Mol. Med. (*in press*).

Cao, H., Weller, S., Orth, J. D., Chen, J., Huang, B., Chen, J. L., Stamnes, M., and McNiven, M. A. (2005). Actin and Arf1-dependent recruitment of a cortactin-dynamin complex to the Golgi regulates post-Golgi transport. Nat. Cell Biol. *7*, 483–492.

Cavallaro, U., and Christofori, G. (2004). Cell adhesion and signalling by cadherins and Ig-CAMs in cancer. Nat. Rev. Cancer *4*, 118–132.

Cho, K. A., Ryu, S. J., Park, J. S., Jang, I. S., Ahn, J. S., Kim, K. T., and Park, S. C. (2003). Senescent phenotype can be reversed by reduction of caveolin status. J. Biol. Chem. *278*, 27789–27795.

D'Souza-Schorey, C. (2005). Disassembling adherens junctions: breaking up is hard to do. Trends Cell Biol. *15*, 19–26.

Engelman, J. A., Chu, C., Lin, A., Jo, H., Ikezu, T., Okamoto, T., Kohtz, D. S., and Lisanti, M. P. (1998). Caveolin-mediated regulation of signaling along the p42/44 MAP kinase cascade in vivo. A role for the caveolin-scaffolding domain. FEBS Lett. *428*, 205–211.

Freelove, R., and Walling, A. D. (2006). Pancreatic cancer: diagnosis and management. Am. Fam. Physician *73*, 485–492.

Fujita, Y., Krause, G., Scheffner, M., Zechner, D., Leddy, H. E., Behrens, J., Sommer, T., and Birchmeier, W. (2002). Hakai, a c-Cbl-like protein, ubiquitinates and induces endocytosis of the E-cadherin complex. Nat. Cell Biol. *4*, 222–231.

Furuyama, H., Arii, S., Mori, A., and Imamura, M. (2000). Role of E-cadherin in peritoneal dissemination of the pancreatic cancer cell line, panc-1, through regulation of cell to cell contact. Cancer Lett. *157*, 201–209.

Garcea, G., Neal, C. P., Pattenden, C. J., Steward, W. P., and Berry, D. P. (2005). Molecular prognostic markers in pancreatic cancer: a systematic review. Eur. J. Cancer *41*, 2213–2236.

Goetz, J. G., Lajoie, P., Wiseman, S. M., and Nabi, I. R. (2008). Caveolin-1 in tumor progression: the good, the bad and the ugly. Cancer Metastasis Rev. *27*, 715–735.

Grande-Garcia, A., Echarri, A., de Rooij, J., Alderson, N. B., Waterman-Storer, C. M., Valdivielso, J. M., and del Pozo, M. A. (2007). Caveolin-1 regulates cell polarization and directional migration through Src kinase and Rho GTPases. J. Cell Biol. *177*, 683–694.

Gumbiner, B. M. (2005). Regulation of cadherin-mediated adhesion in morphogenesis. Nat. Rev. Mol. Cell. Biol. *6*, 622–634.

Henley, J. R., Krueger, E. W., Oswald, B. J., and McNiven, M. A. (1998). Dynamin-mediated internalization of caveolae. J. Cell Biol. *141*, 85–99.

Henley, J. R., and McNiven, M. A. (1996). Association of a dynamin-like protein with the Golgi apparatus in mammalian cells. J. Cell Biol. *133*, 761–775.

Hogan, B. L., and Kolodziej, P. A. (2002). Organogenesis: molecular mechanisms of tubulogenesis. Nat. Rev. Genet. *3*, 513–523.

Imamichi, Y., Konig, A., Gress, T., and Menke, A. (2007). Collagen type I-induced Smad-interacting protein 1 expression downregulates E-cadherin in pancreatic cancer. Oncogene *26*, 2381–2385.

Ivanov, A. I., Nusrat, A., and Parkos, C. A. (2005). Endocytosis of the apical junctional complex: mechanisms and possible roles in regulation of epithelial barriers. Bioessays *27*, 356–365.

Janda, E., Nevolo, M., Lehmann, K., Downward, J., Beug, H., and Grieco, M. (2006). Raf plus TGFbeta-dependent EMT is initiated by endocytosis and lysosomal degradation of E-cadherin. Oncogene *25*, 7117–7130.

Jemal, A., Siegel, R., Ward, E., Murray, T., Xu, J., Smigal, C., and Thun, M. J. (2006). Cancer statistics, 2006. CA Cancer J. Clin. *56*, 106–130.

Joshi, B., *et al.* (2008). Phosphorylated caveolin-1 regulates Rho/ROCK-dependent focal adhesion dynamics and tumor cell migration and invasion. Cancer Res. *68*, 8210–8220.

Karayiannakis, A. J., Syrigos, K. N., Polychronidis, A., and Simopoulos, C. (2001). Expression patterns of alpha-, beta- and gamma-catenin in pancreatic cancer: correlation with E-cadherin expression, pathological features and prognosis. Anticancer Res. *21*, 4127–4134.

Korc, M., Chandrasekar, B., Yamanaka, Y., Friess, H., Buchier, M., and Beger, H. G. (1992). Overexpression of the epidermal growth factor receptor in human pancreatic cancer is associated with concomitant increases in the levels of epidermal growth factor and transforming growth factor alpha. J. Clin. Invest. *90*, 1352–1360.

Korc, M., Meltzer, P., and Trent, J. (1986). Enhanced expression of epidermal growth factor receptor correlates with alterations of chromosome 7 in human pancreatic cancer. Proc. Natl. Acad. Sci. USA *83*, 5141–5144.

Lee, H., *et al.* (2000). Constitutive and growth factor-regulated phosphorylation of caveolin-1 occurs at the same site (Tyr-14) in vivo: identification of a c-Src/Cav-1/Grb7 signaling cassette. Mol. Endocrinol. *14*, 1750–1775.

Li, S., Seitz, R., and Lisanti, M. P. (1996). Phosphorylation of caveolin by src tyrosine kinases. The alpha-isoform of caveolin is selectively phosphorylated by v-Src in vivo. J. Biol. Chem. *271*, 3863–3868.

Lin, M., DiVito, M. M., Merajver, S. D., Boyanapalli, M., and van Golen, K. L. (2005). Regulation of pancreatic cancer cell migration and invasion by RhoC GTPase and caveolin-1. Mol. Cancer *4*, 21–34.

Liu, N., Furukawa, T., Kobari, M., and Tsao, M. S. (1998). Comparative phenotypic studies of duct epithelial cell lines derived from normal human pancreas and pancreatic carcinoma. Am. J. Pathol. *153*, 263–269.

Liu, P., Rudick, M., and Anderson, R. G. (2002). Multiple functions of caveolin-1. J. Biol. Chem. *277*, 41295–41298.

Lu, Z., Ghosh, S., Wang, Z., and Hunter, T. (2003). Downregulation of caveolin-1 function by EGF leads to the loss of E-cadherin, increased transcriptional activity of beta-catenin, and enhanced tumor cell invasion. Cancer Cell *4*, 499–515.

Lubarsky, B., and Krasnow, M. A. (2003). Tube morphogenesis: making and shaping biological tubes. Cell *112*, 19–28.

Menke, A., Philippi, C., Vogelmann, R., Seidel, B., Lutz, M. P., Adler, G., and Wedlich, D. (2001). Down-regulation of E-cadherin gene expression by collagen type I and type III in pancreatic cancer cell lines. Cancer Res. *61*, 3508–3517.

Navarro, A., Anand-Apte, B., and Parat, M. O. (2004). A role for caveolae in cell migration. FASEB J. *18*, 1801–1811.

Oikawa, T., Hitomi, J., Kono, A., Kaneko, E., and Yamaguchi, K. (1995). Frequent expression of genes for receptor tyrosine kinases and their ligands in human pancreatic cancer cells. Int. J. Pancreatol. *18*, 15–23.

Orlichenko, L., Huang, B., Krueger, E., and McNiven, M. A. (2006). Epithelial growth factor-induced phosphorylation of caveolin 1 at tyrosine 14 stimulates caveolae formation in epithelial cells. J. Biol. Chem. *281*, 4570–4579.

Orth, J. D., Krueger, E. W., Weller, S. G., and McNiven, M. A. (2006). A novel endocytic mechanism of epidermal growth factor receptor sequestration and internalization. Cancer Res. *66*, 3603–3610.

Palacios, F., Price, L., Schweitzer, J., Collard, J. G., and D'Souza-Schorey, C. (2001). An essential role for ARF6-regulated membrane traffic in adherens junction turnover and epithelial cell migration. EMBO J. *20*, 4973–4986.

Palacios, F., Schweitzer, J. K., Boshans, R. L., and D'Souza-Schorey, C. (2002). ARF6-GTP recruits Nm23–H1 to facilitate dynamin-mediated endocytosis during adherens junctions disassembly. Nat. Cell Biol. *4*, 929–936.

Palacios, F., Tushir, J. S., Fujita, Y., and D'Souza-Schorey, C. (2005). Lysosomal targeting of E-cadherin: a unique mechanism for the down-regulation of cell-cell adhesion during epithelial to mesenchymal transitions. Mol. Cell. Biol. *25*, 389–402.

Parton, R. G., Hanzal-Bayer, M., and Hancock, J. F. (2006). Biogenesis of caveolae: a structural model for caveolin-induced domain formation. J. Cell Sci. *119*, 787–796.

Parton, R. G., and Simons, K. (2007). The multiple faces of caveolae. Nat. Rev. Mol. Cell Biol. *8*, 185–194.

Patel, H. H., Murray, F., and Insel, P. A. (2008). Caveolae as organizers of pharmacologically relevant signal transduction molecules. Annu. Rev. Pharmacol. Toxicol. *48*, 359–391.

Pelkmans, L., and Helenius, A. (2002). Endocytosis via caveolae. Traffic *3*, 311–320.

Perez-Moreno, M., Jamora, C., and Fuchs, E. (2003). Sticky business: orchestrating cellular signals at adherens junctions. Cell *112*, 535–548.

Pignatelli, M., Ansari, T. W., Gunter, P., Liu, D., Hirano, S., Takeichi, M., Kloppel, G., and Lemoine, N. R. (1994). Loss of membranous E-cadherin expression in pancreatic cancer: correlation with lymph node metastasis, high grade, and advanced stage. J. Pathol. *174*, 243–248.

Rajasekaran, S. A., Gopal, J., Espineda, C., Ryazantsev, S., Schneeberger, E. E., and Rajasekaran, A. K. (2004). HPAF-II, a cell culture model to study pancreatic epithelial cell structure and function. Pancreas *29*, e77–83.

Shi, X., Friess, H., Kleeff, J., Ozawa, F., and Buchler, M. W. (2001). Pancreatic cancer: factors regulating tumor development, maintenance and metastasis. Pancreatology *1*, 517–524.

Suzuoki, M., *et al.* (2002). Impact of caveolin-1 expression on prognosis of pancreatic ductal adenocarcinoma. Br. J. Cancer *87*, 1140–1144.

Tanase, C. P. (2008). Caveolin-1, a marker for pancreatic cancer diagnosis. Expert Rev. Mol. Diagn. *8*, 395–404.

Thiery, J. P. (2002). Epithelial-mesenchymal transitions in tumour progression. Nat. Rev. Cancer *2*, 442–454.

Toyoda, E., Doi, R., Koizumi, M., Kami, K., Ito, D., Mori, T., Fujimoto, K., Nakajima, S., Wada, M., and Imamura, M. (2005). Analysis of E-, N-cadherin, alpha-, beta-, and gamma-catenin expression in human pancreatic carcinoma cell lines. Pancreas *30*, 168–173.

Van den Eynden, G. G., Van Laere, S. J., Van der Auwera, I., Merajver, S. D., Van Marck, E. A., van Dam, P., Vermeulen, P. B., Dirix, L. Y., and van Golen, K. L. (2006). Overexpression of caveolin-1 and -2 in cell lines and in human samples of inflammatory breast cancer. Breast Cancer Res. Treat. *95*, 219–228.

van Golen, K. L. (2006). Is caveolin-1 a viable therapeutic target to reduce cancer metastasis? Expert. Opin. Ther. Targets *10*, 709–721.

Williams, T. M., Cheung, M. W., Park, D. S., Razani, B., Cohen, A. W., Muller, W. J., Di Vizio, D., Chopra, N. G., Pestell, R. G., and Lisanti, M. P. (2003). Loss of caveolin-1 gene expression accelerates the development of dysplastic mammary lesions in tumor-prone transgenic mice. Mol. Biol. Cell *14*, 1027–1042.

Williams, T. M., and Lisanti, M. P. (2005). Caveolin-1 in oncogenic transformation, cancer, and metastasis. Am. J. Physiol. Cell Physiol. *288*, C494–C506.

Williams, T. M., Medina, F., Badano, I., Hazan, R. B., Hutchinson, J., Muller, W. J., Chopra, N. G., Scherer, P. E., Pestell, R. G., and Lisanti, M. P. (2004). Caveolin-1 gene disruption promotes mammary tumorigenesis and dramatically enhances lung metastasis in vivo. Role of Cav-1 in cell invasiveness and matrix metalloproteinase (MMP-2/9) secretion. J. Biol. Chem. *279*, 51630–51646.

Yamanaka, Y., Friess, H., Kobrin, M. S., Buchler, M., Beger, H. G., and Korc, M. (1993). Coexpression of epidermal growth factor receptor and ligands in human pancreatic cancer is associated with enhanced tumor aggressiveness. Anticancer Res. *13*, 565–569.

Zegers, M. M., O'Brien, L. E., Yu, W., Datta, A., and Mostov, K. E. (2003). Epithelial polarity and tubulogenesis in vitro. Trends Cell Biol. *13*, 169–176.